Chapter 4: Mitochondrial DNA mutations as a cause of AHL

Introduction

Mitochondrial mutations may contribute to AHL (Damdimpopoulos *et al.*, 2002; Fischel-Ghodsian, 1999; Johnson *et al.*, 2001). Many mitochondrial disorders appear late in life (Damdimpopoulos *et al.*, 2002; Fischel-Ghodsian, 1999; Johnson *et al.*, 2001). They tend to affect cell types that are postmitotic, that have high energy requirements, and that are often heavily involved in ion pumping, such as hair cells and spiral ganglion cells in cochlea (Fischel-Ghodsian, 1999). In genetic syndromes associated with mutations in mitochondrial DNA defects often appear in the brain, eye, and ear (Fischel-Ghodsian, 1999). Since mitochondrial DNA (mtDNA) is situated near the major site of reactive oxygen species (ROS) production, it becomes particularly vulnerable to ROS damages (Dirks and Leeuwenburgh, 2002; Harmon, 1956; Fischel-Ghodsian, 1999). In addition, mtDNA is not protected by histones and has more limited repair mechanisms than does nuclear DNA (Fischel-Ghodsian, 1999). While some repair and maintenance mechanisms exist for mtDNA, they are in general limited compared with those for nuclear DNA. Mitochondrial DNA polymerase gamma (*Polg*) has proofreading capability that corrects DNA replication errors resulting from nucleotide misincorporation (Kujoth e*l al.*, 2005; Tissenbaum *et al.*, 2004). In *S. cerevisiae*, a specific point mutation in the exonuclease domain of the *Polg* resulted in decreased proofreading activity, which in turn led to a 200-fold

increase in mtDNA mutation rates (Kujoth e*l al.*, 2005; Tissenbaum *et al.*, 2004). In fact, inherited point mutations can lead to mitochondrial syndromes that may have deafness, such as MELAS (mitochondrial encephalomyopathy, lactic acidosis and stroke-like episodes), MERRF (myoclonic epilepsy and ragged red fibres), and MEADF (myoclonic epilepsy, ataxia and deafness) (Fischel-Ghodsian, 1999). D257A mice were created by introducing a specific point mutation (a D to A amino acid change at residue 257) in the exonuclease domain of DNA polymerase gamma (Figure 4.1) (Kujoth e*l al.*, 2005). Because this mouse model expresses a mtDNA polymerase with decreased proof-reading activity, D257A mice exhibit increased spontaneous mutation rates in mtDNA, which in turn accelerate several aspects of aging, such as hair loss (Figure 4-2) (Kujoth e*l al.*, 2005). To test whether the mtDNA mutations play a causal role in the progression of AHL, I conducted ABR analysis, histological analysis, and gene expression analysis using D257A mice. TUNEL (Terminal deoxynucleotidyl transferase biotin-dUTP nick end labeling) assay was also conducted to test whether apoptosis plays a role in AHL induced by mtDNA mutations.

ABR analysis

To assess hearing impairment, ABR thresholds were measured at 4 kHz, 8 kHz, and 16 kHz. The ABR thresholds for the young wt mice were determined to be 23.0 dB SPL at 4 kHz, 19.0 dB SPL at 8 kHz, and 11.0 dB SPL at 16 kHz, exhibiting normal hearing (Figure 4-3). The ABR thresholds for the young D257A mice were determined to be 22.0 dB SPL at 4 kHz, 18.0 dB SPL at 8 kHz, and 15.0 dB SPL at 16 kHz, exhibiting normal hearing

Figure 4-1. The Polg^{D257A} mouse. The Polg^{D257A} (D257A) transgenic mice were created by introducing a specific point mutation (a D to A amino acid change at residue 257) in the exonuclease domain of DNA polymerase gamma (*Polg*). Because this mouse model expresses a mtDNA polymerase with decreased proof-reading activity, D257A mice exhibit increased spontaneous mutation rates in mtDNA, which in turn accelerate several aspects of aging.

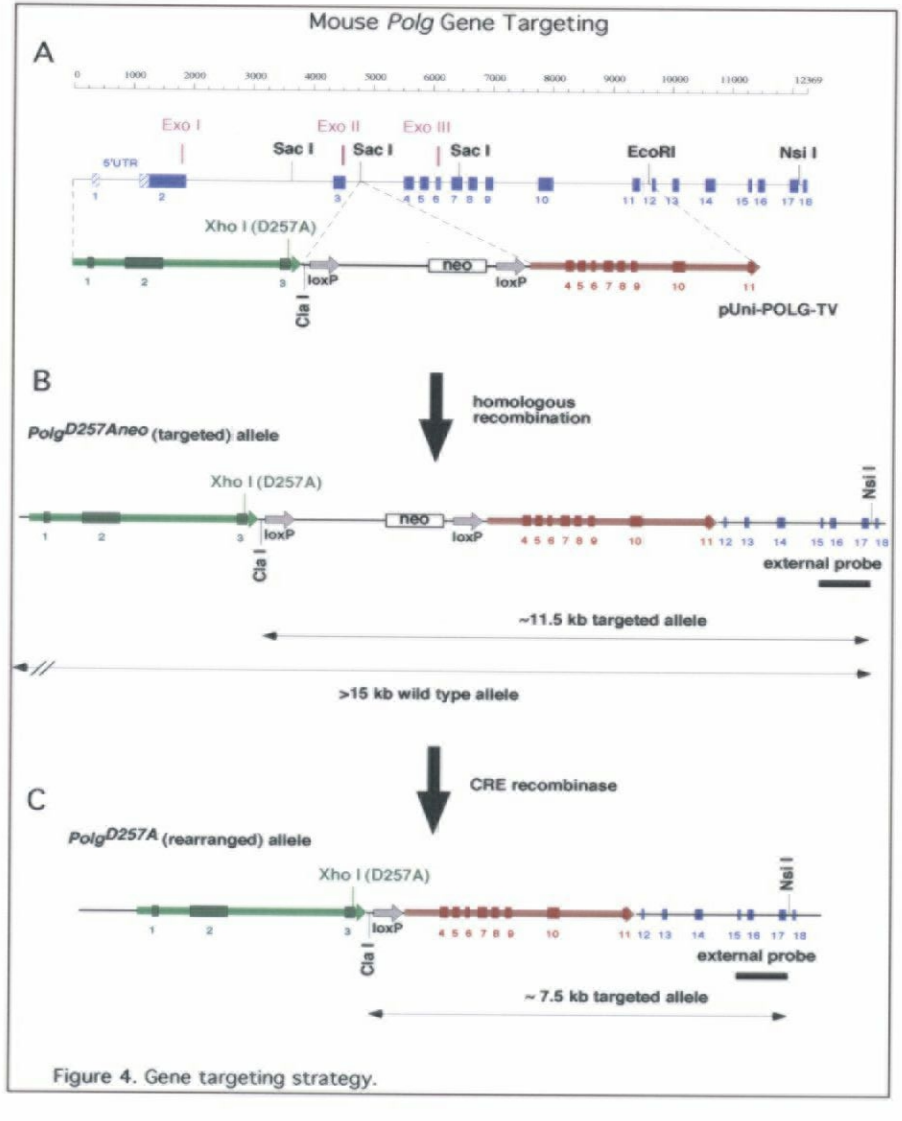

Figure 4. Gene targeting strategy.

Polg^{D257A} Mouse

Polg Gene

Proof-reading activity

↓ **Point Mutation**

Aspartate ⟶ Alanine
at residue 257 in the protein

↓

Decreased proof-reading activity

↓

Increased spontaneous mutation rates in mtDNA

Figure 4-2. $Polg^{D257A}$ mutant exhibiting alopecia. The 12-month-old D257A mouse shows alopecia (hair loss).

1-year-old
wt mouse

Normal hairs

1-year-old
D257A mouse

Loss of hairs

(Figure 4-3). The ABR mean thresholds for the old wt mice were 22.0 dB SPL at 4 kHz, 20.0 dB SPL at 8 kHz, and 13.0 dB SPL at 16 kHz, exhibiting normal hearing (Figure 4-3). The mean of ABR thresholds for the old D257A mice were 52.0 dB SPL at 4 kHz, 41.0 dB SPL at 8 kHz, and 41.0 dB SPL at 16 kHz, exhibiting moderate hearing loss (Figure 4-3). Thus, these results suggest that old D257A mice exhibit AHL, and that mtDNA mutations play a causative role in the progression of AHL.

Histology

Histological analysis revealed that young D257A mice and old wt mice exhibited no degeneration of the organ of Corti, whereas old D257A mice exhibited server loss of spiral ganglion cells and mild loss of hair cells in the cochlea (Figure 4-4). These results support the ABR findings.

Gene expression analysis

To examine transcriptional changes induced by AHL associated with mtDNA mutations, I used oligonucleotide arrays representing 45,037 genes and ESTs. A comparison of the cochlea from the old wt mice and the old D257A mice revealed that AHL induced by mtDNA mutations is associated with significant alterations in mRNA levels. Of the 45,037 genes and ESTs surveyed in the oligonucleotide arrays, we identified 121 genes down-regulated by AHL and 25 genes up-regulated by AHL (Table 4-1). Of the 121 genes that decreased with AHL, 7 genes were hearing-related genes, such as dystonin (*Dst*), reelin (*Reln*), integrin alpha 8 (*Itga8*), otogelin (*Otog*),

Figure 4-3. Comparison of ABR thresholds. ABR thresholds were measured at 4 kHz, 8 kHz, and 16 kHz. The 2-month-old wild-type mice (young wt, n = 5), the 9-month-old wild-type mice (old wt, n = 5), and the 2-month-old mutant mice (young D257A, n = 5) exhibited normal hearing, whereas the 9-month-old mutant mice (old D257A, n = 5) exhibited moderate hearing loss.

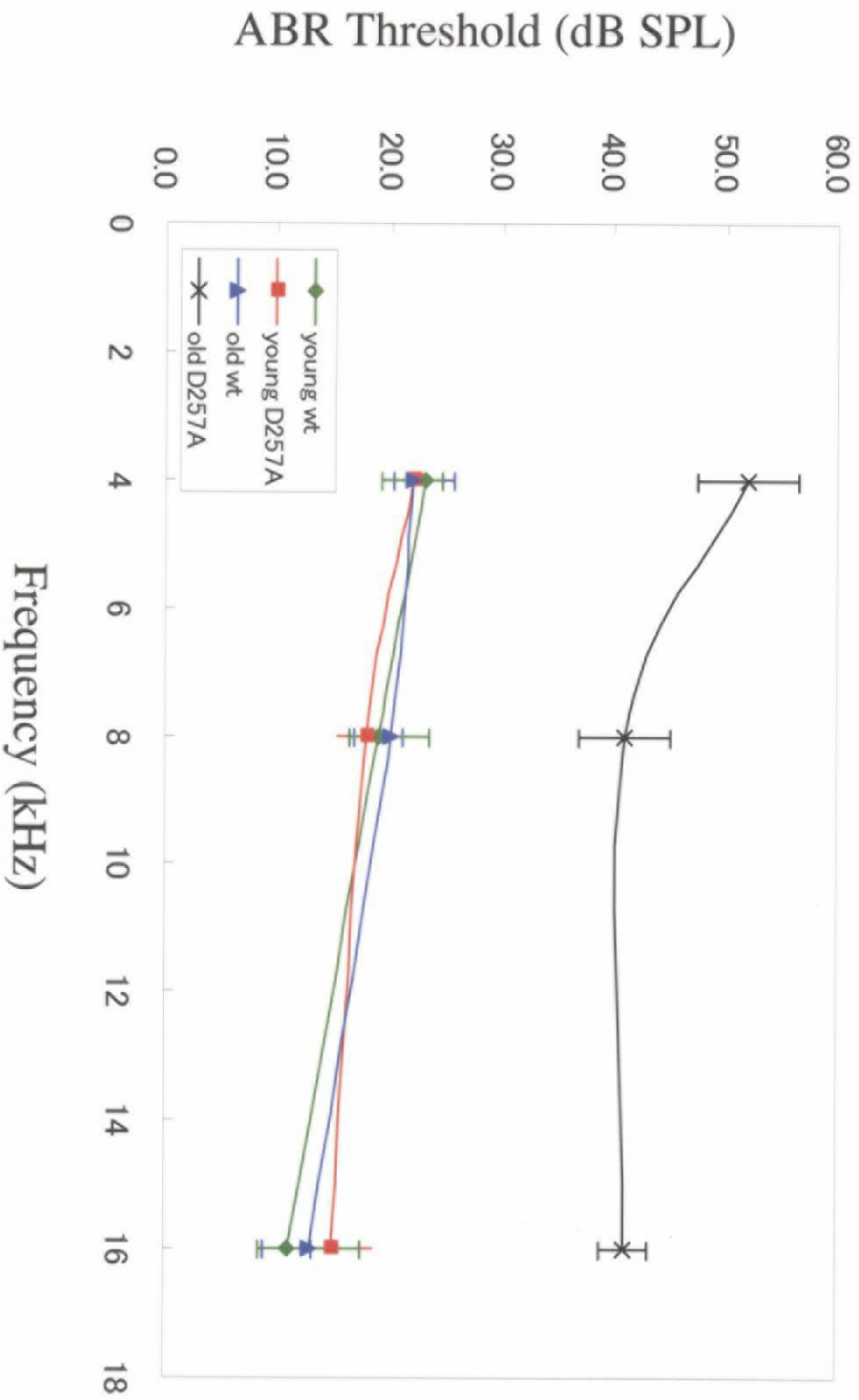
ABR Threshold (dB SPL)
0.0
10.0
20.0
30.0
40.0
50.0
60.0
0
2
4
6
8
10
12
14
16
18
Frequency (kHz)
young wt
young D257A
old wt
old D257A

Figure 4-4. Comparison of cochleae. Representative light micrographs of the lower basal cochlear turn from the 2-month-old mutant mouse (young D257A), the 9-month-old wild-type mouse (old wt), and the 9-month-old mutant mouse (old D257A). The old D257A mouse exhibited severe loss of spiral ganglion cells (SGC) in the cochlea and mild loss of outer hair cells (OHC) and inner hair cells (IHC) in the organ of Corti, whereas the young D257A mouse and the old wt mouse showed no degeneration of the spiral ganglion cells in the cochlea and the organ of Corti.

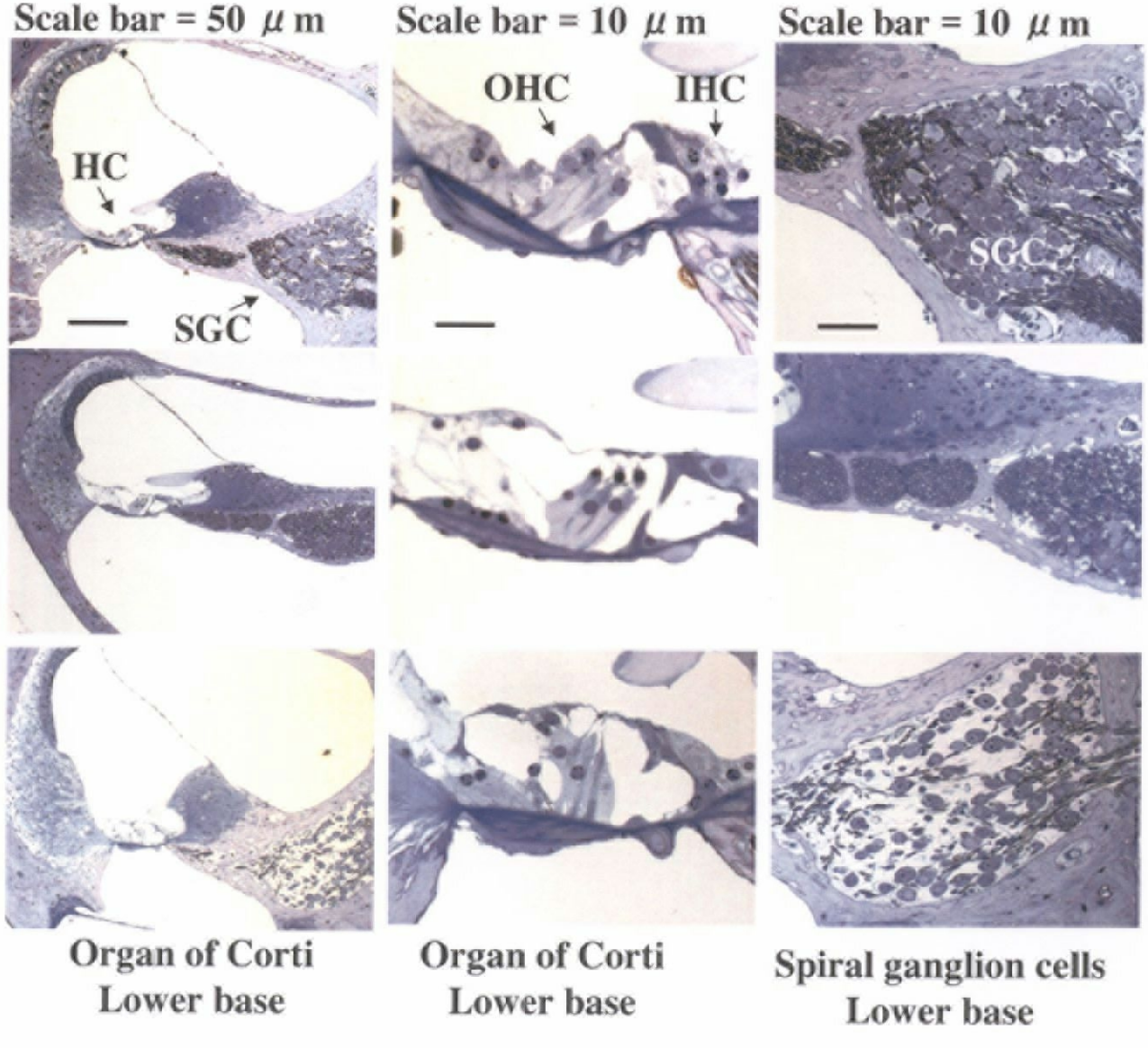
Scale bar = 50 μ m
Scale bar = 10 μ m
Scale bar = 10 μ m
Old wt
(9-month-old)
Young mut
(2-month-old)
Old mut
(9-month-old)
HC
SGC
OHC
IHC
SGC
Organ of Corti
Lower base
Organ of Corti
Lower base
Spiral ganglion cells
Lower base

Table 4-1. List of selected genes altered in the expression by AHL. This table lists genes of selected classes that were significantly (*P* value = 0.01 >, FC = 1.2 ≦) altered in gene expression with AHL. 45,037 genes and ESTs were screened using GeneChips (Mouse Genome 430 2.0). The fold change shown represents the average of all twenty-five possible pairwise comparisons among individual samples (n = 5 for each group) determined using the Microarray Suit Expression Analysis software. GenBank accession numbers are listed under Gene ID.

Gene ID	FC	Gene
Perception of Sound		
AV251091	-6.8	dystonin
NM_011261	-1.7	reelin
BQ175493	-1.6	integrin alpha 8
NM_013624	-1.5	otogelin
AF440694	-1.4	insulin-like growth factor 1
BC025145	-1.4	protein tyrosine phosphatase, receptor type, D
AI385618	-1.3	myelin protein zero
Energy Metabolism		
NM_018870	-13.3	phosphoglycerate mutase 2
NM_007933	-5.8	enolase 3, beta muscle
NM_009943	-4.1	cytochrome c oxidase, subunit VI a, polypeptide 2
BC010758	-2.9	carbonyl reductase 2
BC004589	-1.6	2,3-bisphosphoglycerate mutase
NM_080575	-1.6	acetyl-Coenzyme A synthetase 2 (AMP forming)-like
NM_008062	-1.3	glucose-6-phosphate dehydrogenase X-linked
BC008518	-1.2	nicotinamide nucleotide transhydrogenase
Neurotransmission/Neuronal Factors		
NM_008596	-2.7	mitsugumin 29
BE945884	-2.6	gamma-aminobutyric acid (GABA-A) receptor, subunit alpha 1

(continued)

Gene ID	FC	Gene
NM_013540	-2.0	glutamate receptor, ionotropic, AMPA2 (alpha 2)
BG871810	-1.8	vesicle-associated membrane protein 2
BB130399	-1.7	glutamate receptor, ionotropic, AMPA4 (alpha 4)
BM898651	-1.7	rabphilin 3A
BI143915	-1.7	netrin 1
BQ175666	-1.6	gamma-aminobutyric acid (GABA-A) receptor, subunit beta 3
Apoptosis		
BB298208	3.4	checkpoint kinase 1 homolog (S. pombe)
NM_008960	2.1	phosphatase and tensin homolog
BM120925	1.7	BCL2-like 11 (apoptosis facilitator)
NM_011361	1.6	serum/glucocorticoid regulated kinase
AV270812	1.4	programmed cell death 6 interacting protein
L26349	1.3	tumor necrosis factor receptor superfamily, member 1a
NM_026810	1.2	mutL homolog 1 (E. coli)
Stress Response		
NM_011728	1.5	xeroderma pigmentosum, complementation group A
Inflammatory Response/Immune Modulation		
L778841	2.6	lysosomal trafficking regulator
BG076035	2.3	protein phosphatase 3, catalytic subunit, beta isoform
BF466143	2.2	Wiskott-Aldrich syndrome-like (human)
BG069095	2.1	interferon consensus sequence binding protein 1
NM_134103	2.0	interleukin 1 receptor accessory protein

(*continued*)

Gene ID	FC	Gene
NM_016928	1.6	toll-like receptor 5
BC008167	1.6	interferon activated gene 203
BM234360	1.5	fibronectin 1
BB075261	1.5	Fc receptor, IgG, high affinity I
BE852312	1.3	chemokine-like factor
BC006640	1.3	chemokine (C-X-C motif) ligand 12
NM_021396	1.2	programmed cell death 1 ligand 2
Proteolysis and peptidolysis/Catabolism		
AK013777	2.4	protein tyrosine phosphatase, non-receptor type 21
NM_007800	2.3	cathepsin G
NM_023220	2.0	RIKEN cDNA 2010106G01 gene
NM_008585	1.6	meprin 1 alpha
AK020649	1.4	a disintegrin and metalloproteinase domain 15 (metargidin)
Ion Transport		
NM_020574	-2.5	potassium voltage-gated channel, Isk-related subfamily, gene 3
BG791642	-1.7	ATP-binding cassette, sub-family C (CFTR/MRP), member 9
NM_008557	-1.6	FXYD domain-containing ion transport regulator 3
BM119753	-1.5	potassium voltage-gated channel, shaker-related, subfamily, member 6
AF089751	-1.5	purinergic receptor P2X, ligand-gated ion channel 4
NM_009722	-1.4	ATPase, Ca++ transporting, cardiac muscle, slow twitch 2
BB515151	-1.4	transcobalamin 2
BB553107	-1.3	solute carrier organic anion transporter family, member 2b1

(*continued*)

Gene ID	FC	Gene
Muscle Contraction		
NM_009405	-12.9	troponin I, skeletal, fast 2
NM_011620	-10.4	troponin T3, skeletal, fast
NM_009394	-10.1	troponin C2, fast
AA738859	-9.6	desmin
AJ002522	-8.8	myosin, heavy polypeptide 1, skeletal muscle, adult
BC025172	-8.0	myoglobin
BB474208	-7.9	myomesin 2
NM_007504	-7.8	ATPase, Ca++ transporting, cardiac muscle, fast twitch 1
NM_009608	-7.7	actin, alpha, cardiac
NM_033268	-4.9	actinin alpha 2
NM_009813	-4.9	calsequestrin 1
NM_009416	-3.9	tropomyosin 2, beta
AV209969	-2.5	tropomyosin 1, alpha
NM_013645	-1.8	parvalbumin
NM_009814	-1.8	calsequestrin 2
NM_009722	-1.4	ATPase, Ca++ transporting, cardiac muscle, slow twitch 2
Structure/Structural Modulation		
BC008538	-136.1	myosin, heavy polypeptide 2, skeletal muscle, adult
NM_008469	-23.5	keratin complex 1, acidic, gene 15
NM_007732	-14.0	procollagen, type XVII, alpha 1
AK003182	-7.9	myosin, light polypeptide 1

(*continued*)

Gene ID	FC	Gene
NM_016754	-6.9	myosin light chain, phosphorylatable, fast skeletal muscle
NM_008473	-4.8	keratin complex 2, basic, gene 1
J03458	-4.7	filaggrin
NM_016712	-4.0	tropomodulin 4
BC006780	-3.7	keratin complex 2, basic, gene 5
NM_010861	-3.5	myosin, light polypeptide 2, regulatory, cardiac, slow
U08020	-3.2	procollagen, type I, alpha 1
AK014360	-3.2	keratin complex 1, acidic, gene 10
NM_019645	-3.1	plakophilin 1
AW545978	-2.9	procollagen, type I, alpha 2
NM_011582	-2.9	thrombospondin 4
NM_016798	-2.7	PDZ and LIM domain 3
NM_009675	-2.5	amine oxidase, copper containing 3
NM_016685	-2.3	cartilage oligomeric matrix protein
NM_019759	-2.1	dermatopontin
BI110565	-2.0	periostin, osteoblast specific factor
NM_008476	-1.9	keratin complex 2, basic, gene 6a
BG968894	-1.9	procollagen, type III, alpha 1
NM_009610	-1.8	actin, gamma 2, smooth muscle, enteric
NM_007737	-1.6	procollagen, type V, alpha 2
BM900139	-1.6	RIKEN cDNA D930036B08 gene
AK003780	-1.5	tensin

(*continued*)

Gene ID	FC	Gene
BF451748	-1.4	myosin, light polypeptide kinase
BF158638	-1.4	procollagen, type IV, alpha 1
BB776961	-1.3	cadherin 13
AF064749	-1.3	procollagen, type VI, alpha 3
J03484	-1.3	laminin, gamma 1
AF011450	-1.3	procollagen, type XV
BC021876	-1.2	F11 receptor
Growth Factors/Development		
NM_008780	-5.3	paired box gene 1
NM_009833	-2.6	cyclin T1
NM_009144	-2.3	secreted frizzled-related sequence protein 2
AF100171	-2.2	myeloid leukemia factor 1
AA419994	-2.0	zinc finger protein 145
NM_011641	-1.9	transformation related protein 63
NM_013645	-1.8	parvalbumin
U41739	-1.8	four and a half LIM domains 1
NM_010656	-1.7	sarcospan
BB740660	-1.6	spectrin alpha 1
BG065679	-1.5	protein phosphatase 6, catalytic subunit
BC005486	-1.5	E26 avian leukemia oncogene 2, 3' domain
NM_016910	-1.5	protein phosphatase 1D magnesium-dependent, delta isoform
NM_053015	-1.5	melanophilin

(*continued*)

Gene ID	FC	Gene
BF225802	-1.4	insulin-like growth factor binding protein 5
NM_033270	-1.4	E2F transcription factor 6
BG075883	-1.4	par-3 (partitioning defective 3) homolog (C. elegans)
BQ175880	-1.4	cyclin D2
U25633	-1.4	epithelial membrane protein 1
X96585	-1.3	nephroblastoma overexpressed gene
NM_009790	-1.3	calmodulin 1
Biosynthesis		
AK009352	-8.7	integrin beta 1 binding protein 3
NM_080575	-1.6	acetyl-Coenzyme A synthetase 2 (AMP forming)-like
BG067097	-1.5	Hermansky-Pudlak syndrome 5 homolog (human)
NM_019998	-1.4	asparagine-linked glycosylation 2 homolog (yeast, alpha-1,3-mannosyltransferase)
NM_080637	-1.4	expressed in non-metastatic cells 5
NM_007898	-1.3	phenylalkylamine Ca2+ antagonist (emopamil) binding protein
DNA Synthesis/DNA Repair		
AV301324	-1.8	ribonucleotide reductase M2
Y07687	-1.8	nuclear factor I/B
BB550758	-1.4	progressive external ophthalmoplegia 1 (human)
BG094331	-1.4	polymerase (DNA directed), beta
NM_011951	-1.3	mitogen activated protein kinase 14
NM_015735	-1.3	damage specific DNA binding protein 1
AW556347	-1.2	checkpoint supressor 1

(*continued*)

Gene ID	FC	Gene
Protein Synthesis/Modification		
BC006682	-1.3	eukaryotic translation initiation factor 2, subunit 3, structural gene X-linked
NM_026322	-1.2	methionine sulfoxide reductase A
Fatty Acid Metabolism		
BG793484	-7.3	ankyrin repeat domain 23
AB022340	-4.1	SA rat hypertension-associated homolog
NM_009605	-3.0	adipocyte, C1Q and collagen domain containing
BC007474	-2.4	stearoyl-Coenzyme A desaturase 1
NM_023737	-1.6	enoyl-Coenzyme A, hydratase/3-hydroxyacyl Coenzyme A dehydrogenase

and insulin-like growth factor 1 (*Igf1*). These results were consistent with those of the ABR analysis and the histology analysis. The gene with the largest downregulation in this transcriptional class was Dst gene (fold change = -6.8). This gene encodes cytoskeletal cross-linker protein that connects cytoskeletal elements to cellular junctions and the extracellular matrix (Repentigny *et al.*, 2003). Loss of function of Dst protein within neurons leads to a loss in the maintenance of cytoskeletal organization and to a severe sensory neuropathy including hearing loss (Repentigny *et al.*, 2003). Otog protein is a component of the tectorial membrane in the cochlea, which is involved in the mechanotransduction process (Simmler *et al.*, 2000; Cohen-Salmon et al., 1997). Otog is likely to have a role in the resistance of the tectorial membrane to sound stimulation (Simmler *et al.*, 2000; Cohen-Salmon et al., 1997). Mutations in this gene are thought to cause deafness (Simmler *et al.*, 2000). Igf1 protein has an important role during nervous system development and in its functional maintenance (Varela-Nieto *et al.*, 2004). Mice lacking Ifg1 lose many auditory neurons and exhibit increased auditory thresholds at early postnatal ages (Varela-Nieto *et al.*, 2004). Neuronal loss associated to IGF-I deficiency is caused by apoptosis of the auditory neurons, which presented abnormally increased levels of activated caspase-3 (Varela-Nieto *et al.*, 2004; Shimokawa *et al.*, 2002). Eight genes involved in energy metabolism, such as phosphoglycerate mutase 2 (*Pgam2*), cytochrome c oxidase, subunit VI a, polypeptide 2 (*Cox6a2*), and 2,3-bisphophoglycerate mutase (*Bpgm*), acetyl-Coenzyme A synthetase 2 (AMP forming)-like (*Acas2l*), and glucose-6phosphate

dehydrogenase X-linked (*G6pdx*), also displayed a decrease in the gene expression. These results correlate well with the studies of mitochondria mutations and hearing loss, which show that mitochondrial dysfunction may be associated with AHL (Damdimpopoulos *et al.*, 2002; Fischel-Ghodsian, 1999; Johnson *et al.*, 2001). The gene with the largest downregulation in this transcriptional class was Pgam2 gene (fold change = -13.3). Pgam2 enzyme is involved in glycolsis (Zhang *et al.*, 2001). Cox6a2 protein is involved in cytochrome c oxidase activity in the mitochondria (Mootha *et al.*, 2003), and Acasa2l protein is involved in acetyl-Coenzyme A biosynthesis activity in mitochondria (Beigneux *et al.*, 2004). AHL also lowered the gene expression of eight neurotransmission-related genes including mitsugumin 29 (*Mg29*), gamma-aminobutyric acid (GABA-A) receptor, subunit alpha 1 (*Gabra1*), and glutamate receptor, ionotropic, AMPA2 (alpha 2) (*Gria2*). The gene with the largest downregulation in this transcriptional class was Mg29 gene (fold change = -2.7). Mg29 protein is a member of the synaptophysin family, and is distributed in intracellular membranes including synaptic vesicles (Shimuta *et al.*, 1998; Nishi *et al.*, 1999).

AHL induced 7 apoptosis-related genes, including Checkpoint kinase 1 homolog (*S. pombe*) (*Chek1*), BCL2-like 11 (apoptosis facilitator) (*Bcl2l11*), programmed cell death 6 interacting protein (*Pdcd6ip*), and tumor necrosis factor receptor superfamily, member 1a (*Tnfrsf1a*). These results were consistent with the histological findings. These results also correlate well with the studies of apoptosis and AHL, which show that apoptosis may be

associated with AHL (Fischel-Ghodsian, 1999). The gene with the largest upregulation in this transcriptional class was Chek1 gene (fold change = 3.4). p53 activation is initiated by DNA damage (Prives and Hall, 1999; Vogelstein *et al.*, 2000). This DNA damage is sensed by checkpoint proteins such as Chek1 (Vogelstein *et al.*, 2000; Prives and Hall, 1999). The kinase, Chek1 activates p53 by phosphorylating at amino-terminal sites that are close to the Mdm2-binding region of the protein, thereby blocking its interaction with Mdm2, and leading to activation of p53 (Vogelstein *et al.*, 2000; Urist *et al.*, 2004). Apoptosis can be triggered by members of the Bcl-2 protein family, such as Bcl2l11 (Gross *et al.*, 1999; O'Connor *et al.*, 1998; Bigelow *et al.*, 2004). p53 induces apoptosis through transactivation of the Bcl2l11 genes (Gross *et al.*, 1999; O'Connor *et al.*, 1998). p53 also induces apoptosis through transactivation of members of the TNF receptor family such as Tnfrsf1a (Inagaki-Ohara *et al.*, 2001). AHL induced the gene expression of 12 inflammatory response-related genes including lysosomal trafficking regulator, protein phosphatase 3, interferon consensus sequence binding protein 1, and interleukin 1 receptor accessory protein. These results were also consistent with the histological findings since severe degeneration of cells was found in the old D257A cochlea. AHL also induced the gene expression of 5 proteolysis-related genes, including protein tyrosine phosphatase, non-receptor type 21, chathepsin G, and meprin 1 alpha.

AHL lowered the gene expression of 8 ion transport-related genes including potassium voltage-gated channel, Isk-related subfamily, gene 3,

Figure 4-5. Apoptotic analysis in the mutant cochlea. The TUNEL (Terminal deoxynucleotidyl transferase biotin-dUTP nick end labeling)-positive cells were found in spiral ganglion cells in the 2-month-old mutant mice (young D257A), but not in the 2-month-old wild-type mice (young wt).

Scale bar = 50 μ m

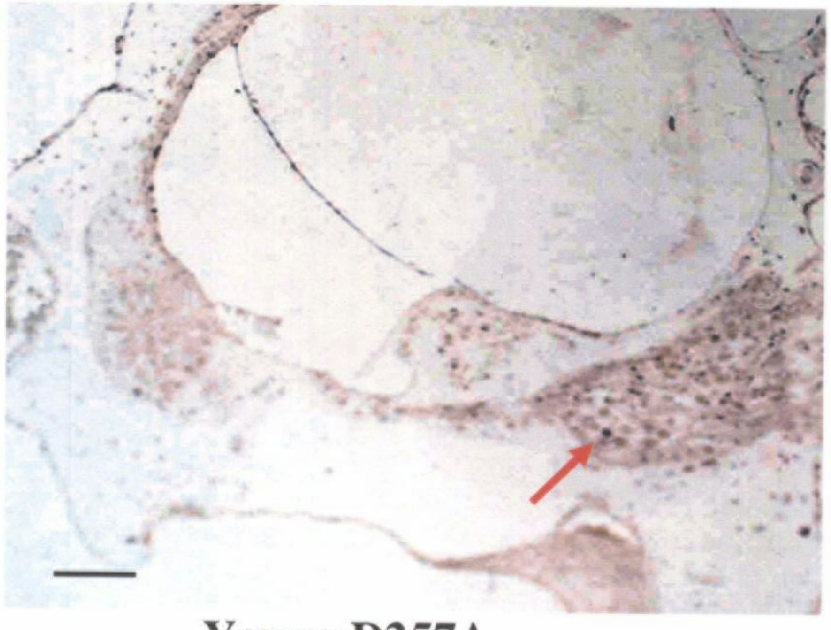

Young D257A
Organ of Corti (lower base)

Scale bar = 10 μ m

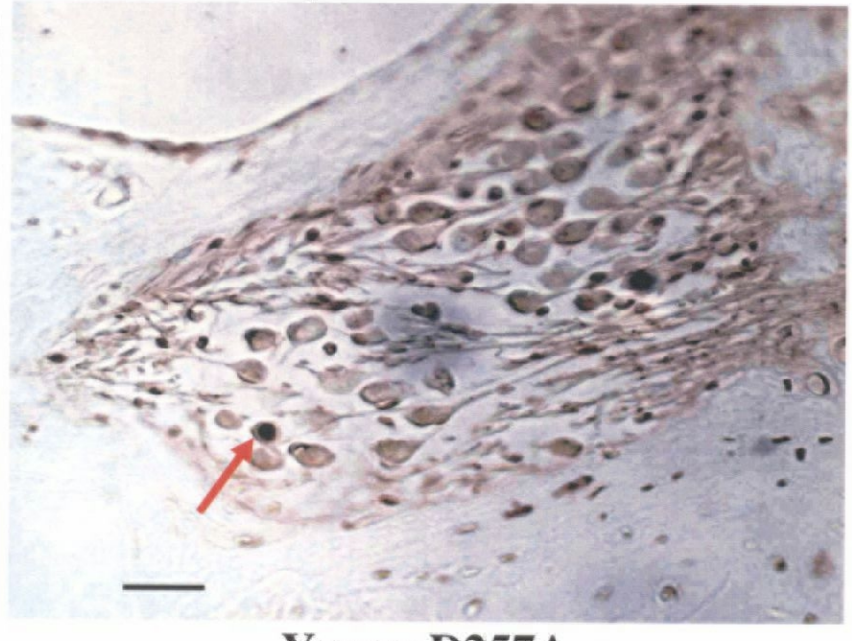

Young D257A
Spiral ganglion cells (lower base)

Table 4-2. Global view of transcriptional changes induced by mtDNA mutations. AHL induced by mtDNA mutations resulted in significant transcriptional changes.

Function	FC	Description
Perception of Sound	↓	Suppression of hearing-related genes
Energy metabolism	↓	Mitochondrial dysfunction, Reduced glycolysis
Neurotransmission/Neuronal Factors	↓	Decreased neurotransmitter transport, neurogenesis
Apoptosis	↑	Induction of apoptosis
Stress Response	↑	Induction of oxidative stress-inducible genes
Inflammatory Response	↑	Induction of inflammatory response, immune response
Proteolysis and Peptidolysis	↑	Increased proteolysis and peptidolysis
Ion Transport	↓	Decreased potassium ion transport, sodium ion transport,
Muscle Contraction/Muscle Modulation	↓	Suppression of muscle contraction and muscle development
Structure/Structural Modulation	↓	Suppression of cytoskeleton organization and cell adhesion
Growth Factors/Development	↓	Suppression of cell growth and cell differentiation
Biosynthesis	↓	Decreased glycolipid biosynthesis and prostaglandin biosynthesis
DNA Synthesis/DNA Repair	↓	Suppression of DNA replication factors and DNA repair factors
Protein Synthesis/Modification	↓	Decreased protein biosynthesis and protein modification
Fatty Acid Metabolism	↓	Reduced fatty acid biosynthesis

ATP-binding cassette, sub-family C (CFTR/MRP), and member 9, and potassium voltage-gated channel, shaker-related subfamily, member 6. AHL also lowered transcripts associated with muscle contraction, such as troponin I, skeletal, fast 2, troponin T3, skeketak, fast, and troponin C2, fast. AHL was characterized by reductions in the gene expression of structural modulation, growth factor, biosynthesis, DNA synthesis, DNA repair, protein synthesis, and fatty acid metabolism.

TUNEL assay

The TUNEL assay results revealed that TUNEL-positive cells were found in spiral ganglion cells in the cochlea of the young D257A mice, but not in the young wt mice (Figure 4-5). This result indicates that apoptosis plays a role in the progression of AHL.

Summary of findings

The ABR results and histological results showed that old D257A mice exhibited AHL, suggesting that mtDNA mutations play a causative role in the progression of AHL. A summary of global view of transcriptional changes induced by AHL associated with mtDNA mutations is shown in Table 4-2. These results revealed that the transcriptional changes induced by AHL associated with mtDNA mutations were consistent with those of the DBA mouse study. AHL induced by mtDNA muttions resulted in suppression of hearing-related genes, decreased energy metabolism, and induction of apoptosis-related gene, including *Chek1*, *Bcl2l11*, and *Tnfrsf1a*, which

mediate p53-dpendent apoptosis (Vogelstein *et al.*, 2000; Prives and Hall, 1999; Urist *et a*l., 2004; Gross *et al.*, 1999; O'Connor *et al.*, 1998; Bigelow *et al.*, 2004; Inagaki-Ohara *et al.*, 2001). The TUNEL result suggests that apoptosis plays a role in the progression of AHL. Mitochondrial DNA damage can induce Chek1 gene, which in turn activates p53-dependent apoptosis. Taken together, these suggest that AHL develops by mechanisms that may be related to induction of apoptosis by mitochondrial dysfunction.